

₁ Covariance of Meiyu Front and Tropospheric Jet ₂ Variability on Daily and Interannual time scales

Jesse A. Day,¹ Jacob Edman,¹ Inez Fung¹, and Weihan Liu¹

Corresponding author: Jesse Day, University of California Berkeley, Department of Earth and Planetary Science, College of Letters and Science; 307 McCone Hall, Berkeley, CA 94720, USA.
(jessed@berkeley.edu)

¹Department of Earth and Planetary
Science, University of California Berkeley,
Berkeley, California, USA.

- ³ This abstract must be 150 words or less. The contents of the abstract count
- ⁴ towards the total word count.

1. Introduction

China receives about 60% of its rainfall from May to August, known collectively as the East Asian summer monsoon. The period of peak rainfall within this monsoon features a northward-migrating front known as the Meiyu front (lit. “Plum rains” – capitalize front?), and lasts roughly from early June to mid-July (“Meiyu Season”). A growing volume of evidence suggests a shift in mean rainfall patterns over China beginning in the late 1970s, with increased flooding in the south and droughts in the north (the “South Flood North Drought”). A permanent change would have major humanitarian impacts on the densely-populated eastern Chinese plain, where a sizable fraction of the population depends on agriculture. The Chinese government has already embarked on a costly engineering project to reroute water from the Yangtze to the Yellow River, the South-North Water Transfer Project.

The complex atmospheric dynamics of the East Asian summer monsoon remain a source of debate [*Sampe and Xie*, 2010; *Chen and Bordoni*, 2014]. The behavior of the Meiyu front has been discussed in the seasonal mean [*Ding and Chan*, 2005], and in relation to interannual rainfall variability [?]. However, to our knowledge, no comprehensive statistics of daily Meiyu behavior exist. We have developed an algorithm to compile a 57-year climatology (1951-2007) of frontal events in China (hereafter referred to as Meiyu events) based on the APHRODITE rain gauge product. In addition, we test the covariance of daily Meiyu behavior with that of the tropospheric jet, using an existing database from *Schiemann et al.* [2009]. Past work has compared jet and Meiyu variability over shorter time periods or with coarse resolution *Liang and Wang* [1998], but none has systematically

compared the two. Finally, given our daily Meiyu climatology, we determine whether there are apparent changes in behavior over the 57 years, and whether these also correspond to changes in jet behavior.

2. Data sets

The analysis contained in this paper relies on two data sets, APHRODITE and Schiemann et al.'s database of jet counts. APHRODITE (Asian Precipitation - Highly-Resolved Observational Data Integration Towards Evaluation of the Water Resources) [Yatagai et al., 2012]. The APHRO_MA_V1101 product includes 57 years (1951-2007) of daily precipitation (PRECIP product, units mm day⁻¹) and station coverage (RSTN product) on a .25° × .25° grid (roughly 25 km spacing) between 60°E-150°E and 15°S-55°N. We focus on the subregion from 100E-123E and 20N-40N as the area of occurrence of Meiyu events. Rain gauge products present an analytical challenge because the distribution of stations is uneven in space and changes with time. Station density over eastern China improves beginning in the 1970s from X to Y (INSERT ACTUAL NUMBERS). However, the spacing of stations generally does not exceed 100 km, which should be more than sufficient to resolve the macroscopic scale of a frontal event.

For tropospheric jet variability, we employ a database based on ERA-40 reanalysis data developed by Schiemann et al. [2009]. Their database includes every appearance of a tropospheric jet in East Asia for 1958-2001 at 6-hourly intervals using simple criteria: Positive zonal wind and local maximum in excess of 30 m/s. We have modified Schiemann et al.'s algorithm in several respects: ...

3. Meiyu Climatology

3.1. Algorithm

For each day from 1 January 1951 to 31 December 2007 (20,819 total), our Meiyu algorithm determines. In addition, some days feature two frontal events, each of which are separately detected. The algorithm follows the subsequent checklist:

1. At each longitude, we find the latitude .We find the lat If a 5°swath (20 points) of maxima exceeds 10 mm/day, we move to step 2. Otherwise it is a no-Meiyu day.

2. Given a preliminary fit, we perform a weighted least-squares linear fit of the *latitudes* with the intensity as weight.

3. A recursive algorithm. Using the initial fit as guideline, we select a new set of maxima within k degrees of the best fit line. k is progressively decreased with each iteration.

4. We now have a best fit estimate. This allows us to calculate the “quality score” Q_1 , which equals the fraction of total daily precipitation inside our domain that falls within 5 degrees of our best fit.

5. The algorithm now looks for a secondary front as follows:

- (i) All precipitation within the primary front is removed. The front criterion from Step 1 is repeated. If passed, steps 2-4 are repeated.

- (ii) If a secondary Meiyu is found, we also calculate Q_2 , which is the fraction of precip inside of the secondary front *with primary front removed*, and $Q_{1.alt}$, which is precip frac inside first front *with secondary front removed*.

6. The day is now classified as either a primary Meiyu day, a primary AND secondary Meiyu day, or a no-Meiyu day. We use the following criteria:

(i) We define the “Taiwan fraction” (TW) as the percentage of daily rainfall that falls over Taiwan. If TW \geq 20%, there is no Meiyu. We do this because...

(ii) If $Q_1 > .6$, the primary Meiyu is counted. If there is a secondary front and $Q_2 > .6$, the secondary front is also counted.

(iii) If $Q_1 < .6$, then we check if both Q_{1_alt} and $Q_2 > .6$. In these (rare) cases, both fronts are counted in our statistics. Otherwise, it is a no-Meiyu day. This allows us to find double front days where the original Q_1 was too low.

We develop an adaptive algorithm to detect the position of the Meiyu front on a given day. For each day from 1951 to 2007 (20819 days total), we first find the quantity and latitude of maximum rainfall for each longitude point. Then, we use the simple criterion of there being a 5 degree continuous chain of maxima over 10 mm/day (20 consecutive cells). We then try to linearly fit these maxima, excluding any maximum that is more than 5 degrees of latitude away from the precipitation centroid given by $\langle L \rangle = \frac{\sum P_i y_i}{\sum P}$. Next using, this first fit as starting point, we now find the maxima within a n -degree latitude window of the best fit line, where we progressively shrink n with each iteration. The choice of n does not greatly impact fit quality. In our experiment, we repeated the fit for $n = \dots$. Given a final fit, we report the latitude of the front at 105°E, the mean intensity of rainfall along the center of its axis and the tilt (in degrees). We also report a quality score Q which indicates the percentage of rainfall that falls within 3 degrees of our best fit line, such that statistical calculations can be repeated only days with a clear front for the purpose of confirmation.

3.2. Defining Meiyu season

Figure 1 shows a Hövmoller diagram of latitudes occupied by the Meiyu Front in the 57-year mean. Four local maxima of Meiyu events can be observed: 1) A "pre-Meiyu" from May 1-31 over southern China (Ding and Chan's first position); 2) Meiyu Season, in which the preferred latitude of the front shifts by almost ten degrees from June 1-July 15 (Ding and Chan stage 2); 3) A "post-Meiyu" of persistent 4) Cyclone season over Southern China. The storms during season 4 can be distinguished from earlier Meiyu events in southern China because their propagation direction is westward, opposite to eastward Meiyu storms. The combination of stages 3 and 4 corresponds to the third stage of the Meiyu in Ding and Chan, but only the core of Meiyu season (their stage 2) features significant front migration. Figure 2 shows that even in winter, rainfall events in China tend to be frontal, but their frequency increases up to almost 100% during Meiyu Season, and a surge in intensity can be seen around June 1 where mean rainfall along the front exceeds 25 mm/day. The mean tilt of the front is approximately 8 degrees.

It can be seen that mean rainfall and Meiyu occurrence are not entirely equivalent, since the Southern China peak in August does not correspond to a surge in Meiyu events.

4. Preferred jet positions

The westerly jet and rainfall are argued to covary on paleoclimate timescales [Nagashima *et al.*, 2011][Nagashima *et al.*, 2013].

Monthly changes in the position of the jet have previously been reported in Schiemann *et al.* [2009], and we do not repeat them here. It is worth noting that the pre-Meiyu in May corresponds to a time of great jet variability, whereas June features a discernible but

meandering jet, and the post-Meiyu corresponds to very low variability in jet position during July and August.

Finally, we use our knowledge of daily Meiyu positions to isolate preferred configurations for different dates, as well as probability distributions of the tropospheric jet associated with each configuration. If a robust change in mean jet progression is detected, we may be able to isolate a corresponding shift in Meiyu distribution that may have previously gone unnoticed due to extreme temporal variability in the data.

We first attempt to define a transition date from spring to summer behavior in the jet database, and equivalently from Meiyu Season to post-Meiyu in our new catalog. Preliminary evidence suggests a long-term perturbation in mean jet path in East Asia from the 1960s to present with later onset of summer jet and shorter total duration of summer jet. In our Meiyu database it is more difficult to extract an exact transition date due to high-frequency variability in space and time. However, we observe an apparent shift in the timing of northward progression of the Meiyu Front between 1951-1970 and 1988-2007. If both databases demonstrate a robust decadal shift, they may provide an explanation for the anecdotal South Wet-North Dry pattern of rainfall change.

5. Covariance of jet and Meiyu anomalies

6. Dynamics

The covariance of Meiyu front positions and tropospheric jet latitudes previously demonstrated also clarifies a dynamical reason for their seasonality. As shown, Meiyu season consists of intense rainfall from June 1st to July 1st with a shift in latitude of almost 10 degrees over the course of that month. After . The lens of forced convergence by

the Tibetan Plateau. In the climatological mean, *Chen and Bordonì* [2014] demonstrated that the Meiyu front exists primarily due to forced mechanical convergence by the Tibetan Plateau upstream. They showed this by using experiments in which the Tibetan Plateau's height was reduced by 95%. We argue that our results similarly show the role of the Tibetan Plateau in generating a strong Meiyu front. When the jet impinges on the Tibetan Plateau from late May to early July, the high topography induces meanders that force standing waves in jet configuration, pushing it further north from 80E to 100E and then further south into China. This in turn anchors strong rainfall along the Meiyu front in China. When the jet moves further north to its preferred summer position, which occurs just north of the Tibetan Plateau, it is no longer deflected and the front is significantly weaker, though events do still occur as seen in Figure 1. We confirm this hypothesis by showing the climatology of precipitable water vapor from SSRI from time A, time B, time C and time D (last figure). During the early and late stages of Meiyu season precipitable water content is concentrated along bands that intersect central China. However, in July and August, the latitude of the moisture vapor front has shifted much further north, over northern China, and both the Bay of Bohai and the Korean Peninsula and Japan all have much greater precipitable water. However, the lack of mechanical forcing is shown by the weakness of rainfall in those events (<20 mm/day versus 25-30 mm/day over southern and central China during Meiyu season).

7. Conclusion

Since the behavior of the jet is coupled to global climate variability, our work holds the promise of attributing the regional rainfall trend in China to global-scale change.

Existing templates for precipitation changes under warming ([*Held and Soden*,
2006][*Lintner and Neelin*, 2007][*Chou et al.*, 2009]) are not easily applied to the East
Asian monsoon

Acknowledgments. APHRODITE is...

References

- Chen, J., and S. Bordoni (2014), Orographic Effects of the Tibetan Plateau on the East
Asian Summer Monsoon: An energetic perspective, *J. Climate*, p. 140113153908002,
doi:10.1175/JCLI-D-13-00479.1.
- Chou, C., J. D. Neelin, C.-A. Chen, and J.-Y. Tu (2009), Evaluating the rich-get-richer
mechanism in tropical precipitation change under global warming, *J. Climate*, 22(8),
1982–2005, doi:10.1175/2008JCLI2471.1.
- Ding, Y., and J. C. L. Chan (2005), The East Asian summer monsoon: an overview,
Meteorol. Atmos. Phys., 89(1-4), 117–142, doi:10.1007/s00703-005-0125-z.
- Held, I., and B. Soden (2006), Robust responses of the hydrological cycle to global warm-
ing, *J. Climate*, 19(21), 5686–5699.
- Liang, X., and W. Wang (1998), Associations between China monsoon rainfall and tro-
pospheric jets, *Q. J. R. Meteorol. Soc.*, 124(May), 2597–2623.
- Lintner, B., and J. D. Neelin (2007), A prototype for convective margin shifts, *Geophys.*
Res. Lett., 34(5), L05,812, doi:10.1029/2006GL027305.
- Nagashima, K., R. Tada, A. Tani, Y. Sun, Y. Isozaki, S. Toyoda, and H. Hasegawa (2011),
Millennial-scale oscillations of the westerly jet path during the last glacial period, *J.*

169 *Asian Earth Sci.*, *40*(6), 1214–1220, doi:10.1016/j.jseas.2010.08.010.

170 Nagashima, K., R. Tada, and S. Toyoda (2013), Westerly jet-East Asian summer monsoon
171 connection during the Holocene, *Geochemistry, Geophys. Geosystems*, *14*(12), 5041–
172 5053, doi:10.1002/2013GC004931.

173 Roe, G. (2009), On the interpretation of Chinese loess as a paleoclimate indicator, *Quat.*
174 *Res.*, *71*(2), 150–161, doi:10.1016/j.yqres.2008.09.004.

175 Sampe, T., and S.-P. Xie (2010), Large-Scale Dynamics of the Meiyu-Baiu Rain-
176 band: Environmental Forcing by the Westerly Jet, *J. Climate*, *23*(1), 113–134, doi:
177 10.1175/2009JCLI3128.1.

178 Schiemann, R., D. Lüthi, and C. Schär (2009), Seasonality and Interannual Variability
179 of the Westerly Jet in the Tibetan Plateau Region, *J. Climate*, *22*(11), 2940–2957,
180 doi:10.1175/2008JCLI2625.1.

181 Yatagai, A., K. Kamiguchi, O. Arakawa, A. Hamada, N. Yasutomi, and A. Kitoh (2012),
182 APHRODITE: Constructing a Long-Term Daily Gridded Precipitation Dataset for Asia
183 Based on a Dense Network of Rain Gauges, *Bull. Am. Meteorol. Soc.*, *93*(9), 1401–1415,
184 doi:10.1175/BAMS-D-11-00122.1.

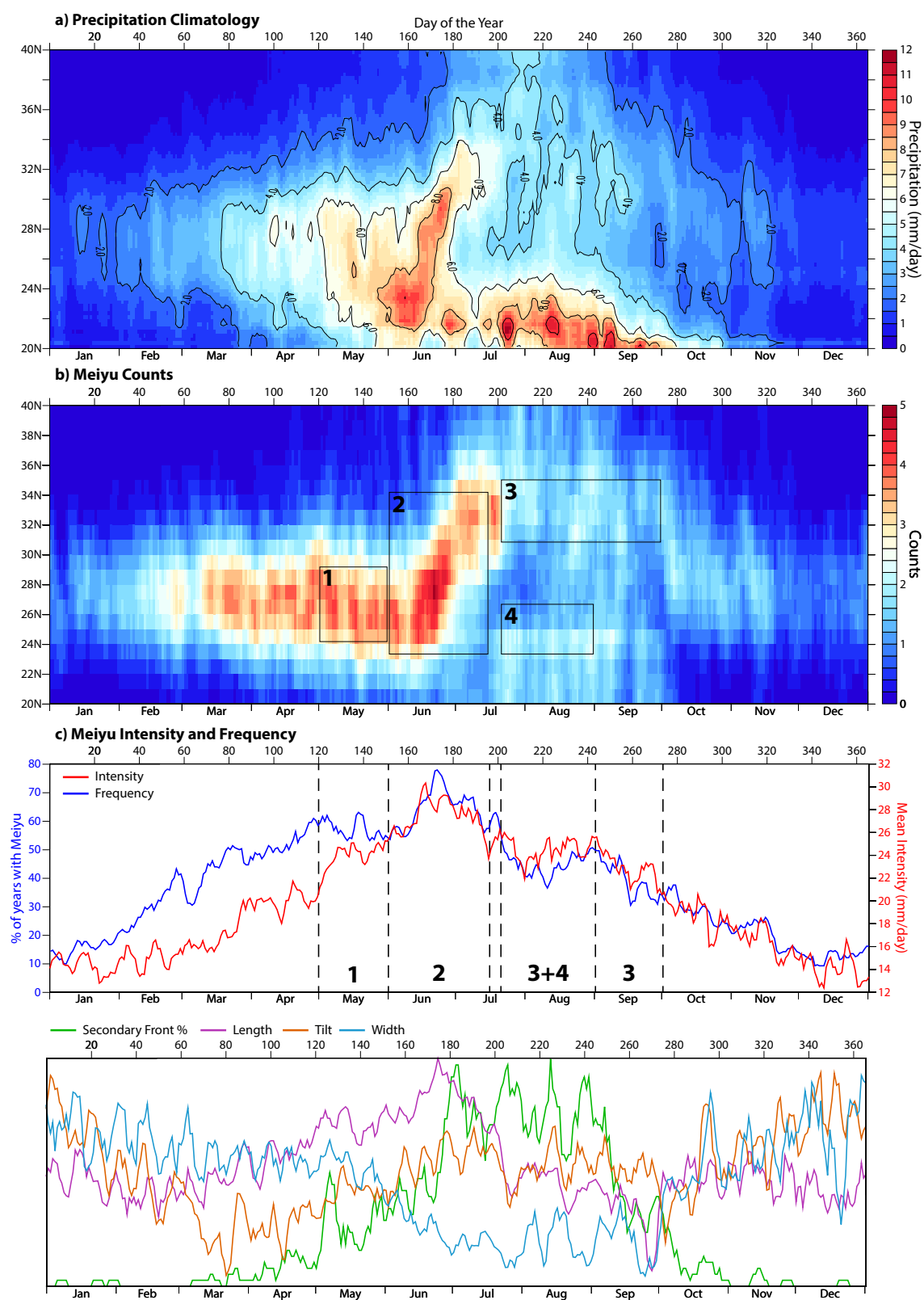


Figure 1. Climatology of the Meiyu Front, 1951-2007. 1) Pre-Meiyu 2) Meiyu 3) Cyclone season in Southern China 4) Storms advected by summer jet

D R A F T September 3, 2014, 12:13pm D R A F T